A FAST AND EFFICIENT ON-LINE HARMONICS ELIMINATION PULSE WIDTH MODULATION FOR VOLTAGE SOURCE INVERTER USING POLYNOMIALS CURVE FITTINGS

Z. Salam

Faculty of Electrical Engineering, Universiti Teknologi Malaysia
UTM 81310 Skudai, Johor Bahru, Johor, Malaysia
zainals@fke.utm.my

(Received: October 9, 2007 – Accepted in Revised Form: November 5, 2009)

Abstract The paper proposes an algorithm to calculate the switching angles using harmonic elimination PWM (HEPWM) scheme for voltage source inverter. The algorithm is based on curve fittings of a certain polynomials functions. The resulting equations require only the addition and multiplication processes; therefore, it can be implemented efficiently on a microprocessor. An extensive angle error analysis is carried out to determine the accuracy of the algorithm in comparison to the exact solution. To verify the workability of the technique, an experimental voltage source inerter was constructed. Since the proposed HEPWM algorithm is simple and fast, it is implemented using a low cost, 16-bit microprocessor.

Keywords Power Electronics, Inverter, Harmonics Elimination Method, Pulse-Width Modulation

چکیده این مقاله الگوریتمی را برای محاسبه زوایای سوییچینگ با استفاده از روش PWM حذف هارمونیک (HEPWM) برای مبدل‌های منبع ولتاژ پیشنهاد می کند. این الگوریتم بر مبنای تطابق منحنی توابع چند جمله‌ای خاص استوار است. معادله حاصل تنها به اعمال جمع و ضرب نیاز دارد، بنابراین آن را می توان با کارآیی بالا برای یک ریزپردازنده به کار برد. یک تجزیه و تحلیل خطای زاویه گسترده برای تعیین دقت این الگوریتم در مقایسه با حل دقیق انجام می شود. برای تایید عملکرد این روش، یک مبدل منبع ولتاژ آزمایشگاهی ساخته شد. چون الگوریتم HEPWM پیشنهادی ساده و سریع است، با استفاده از یک ریزپردازنده ۱۶ بیتی ارزان قیمت به کار برده شد.

1. INTRODUCTION

The application of harmonics elimination concept in pulse width modulation (PWM) for voltage source inverter (VSI) was originally demonstrated by Patel, et al [1,2]. The advantages of HEPWM are widely recognized- the main benefit is its superior harmonics performance compared to the sinusoidal PWM. Other benefits include the reduction of radio frequency interference, torque pulsations and speed ripples. Despite these advantages, there remains one problem that has prevented the widespread use of HEPWM, namely the difficulty to calculate the switching angles online. This is basically due to the fact that the equations to calculate switching angles in a HEPWM scheme are non-linear and transcendental, which will not allow for online calculation using a digital method. As a result, an off line computation need to be carried out using numerical methods such as the Newton-Raphson iteration. This method produces accurate solutions and good convergence provided that the initial guess for the switching angles is near the local minima [3]. However such operation requires massive computational capacity because large iteration cycles are required if the "initial value" is not correctly chosen. Once the set of HEPWM angles are obtained using off-line computers, they are stored in memory on the PWM generator and called upon when the PWM waveform is to be constructed. This method is known as Programmed HEPWM and is a popular approach as documented in [4]. One of the major drawbacks of this technique is the large memory that is required if there are changes in modulation parameters such as the amplitude or frequency ratios. Furthermore or more accurate results, interpolations in-between points may be required.

Research has been carried out to derive the HEPWM switching angle equations to make them

possible for online calculation. The advantage of this approach is clear. First the memory to store the switching angles is no longer required. Second, all the angles can be calculated on-line as demanded by the modulation parameters. It appears that all schemes in this category of HEPWM require some sort of derivation to arrive at a mathematical solution that could be computed using microprocessors. One of the early attempts for such work is carried out by Taufiq, et al [5]. He derived a set of non-transcendental equations for near-optimal solution using sine-wave approximation approach. Using this scheme, the HEPWM switching angles equations are reduced to non-transcendental form that permits for an on-line HEPWM computation using Digital Signal Processor. Another HEPWM scheme, based on regular sampled PWM technique was suggested by Bowes [6]. The same author also carried out similar work for the space vector modulation scheme [7]. The HEPWM scheme using bipolar switching is proposed in [8]. Other more complex methods are proposed by Liang using the Walsh functions [9] and Kato using homotopy-based computation [10]. Chiasson, et al [11] proposed the resultant theory derived a complete solution for the switching angles. The technique is applied to a multilevel inverter structure [12], and further extended to multilevel inverter with non-equal DC sources [13]. More recently HEPWM scheme for multilevel inverter using genetic algorithm is proposed [14].

To implement the on-line HEPWM, it appears that most researchers opted for the digital signal processors (DSP). This is inevitable, as HEPWM algorithms are generally complex and significant computing power is required to calculate the switching angles. For low end inverter system, a low cost microprocessor would be desirable. In this report, a fast and efficient HEPWM scheme based that can be suitably implemented using a low cost fixed point microprocessor is proposed. It is based on the polynomial curve fitting of the trajectories of the exact HEPWM angles. It shall be shown that the proposed scheme allows for an efficient on-time computation but with acceptable error margins. The viability of the scheme will be validated with hardware results.

2. DERIVATION OF NEAR-OPTIMAL HEPWM EQUATIONS

Figure 1 shows a generalized bipolar PWM waveform with M chops per half-cycle. It is assumed that the periodic waveform has half-wave symmetry and unit amplitude. The basic square wave is chopped a number of times and a fixed relationship between the number of chops and possible number of harmonics that can be eliminated is derived. The odd switching angles, $\alpha_1, \alpha_3, \text{etc.}$, define the negative going transitions

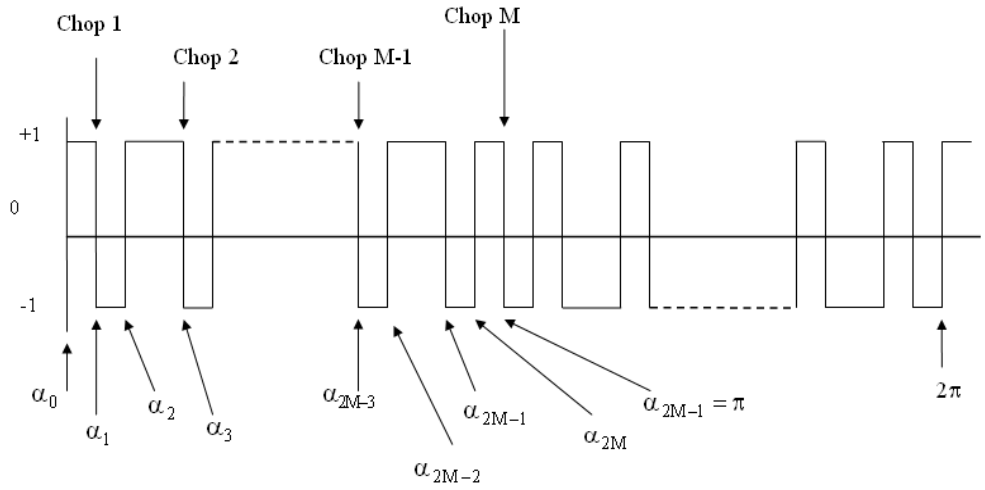

Figure 1. Generalized quarter-wave symmetric PWM waveform.

and the even switching angles, α_2, α_4, etc. define the positive going transitions. As the waveform is quarter-wave symmetric, only odd harmonics exist and are given by the following Fourier series representation:

$$A_n = \frac{4}{n\pi}\left[1 + 2\sum_{k=1}^{m}(-1)^k \cos n\alpha_k\right] \quad (1)$$

$$B_n = 0 \quad (2)$$

Equation 1 has m variables (α_1 to α_m) and a set of solutions is obtainable by equating any m-1 harmonics to zero and assigning a value to the fundamental. Thus both the harmonics incidents and the fundamental components can be independently controlled. These equations are nonlinear as well as transcendental.

The trajectories for the switching angles ($\alpha_1, \alpha_3 ... \alpha_m$) versus the amplitude of the fundamental component of the pole switching waveform (NP1) for odd number of switching per quarter cycle can be obtained by computation. Figures 2a-d show some trajectories calculated for m = 3, 5, 7 and 13, respectively.

From Figures 2a-d the highest intersection point for the trajectories with the y-axis is 60°.

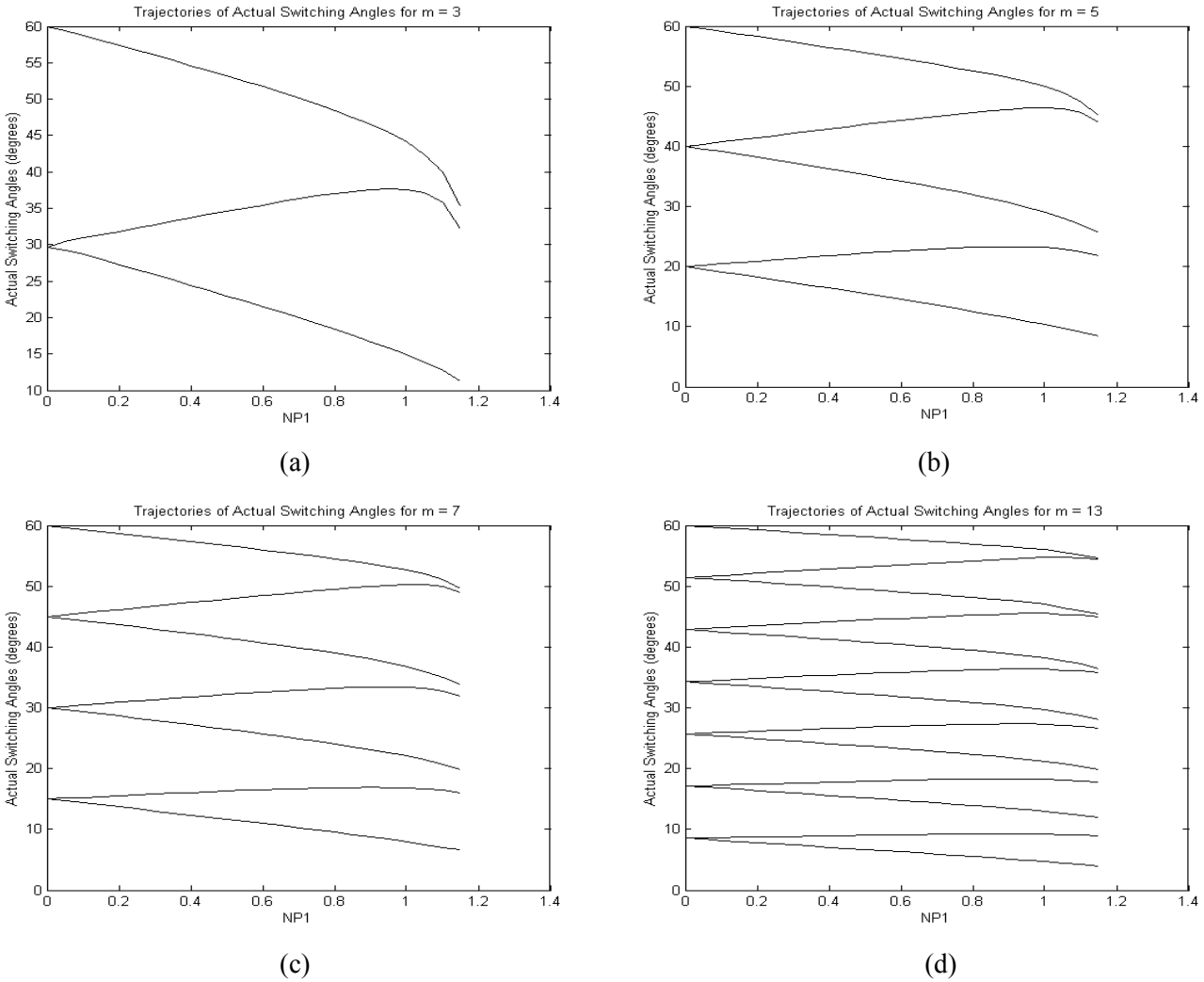

Figure 2. The Trajectories of switching angles for an odd number of switchings per quarter cycle (a) m = 3, (b) m = 5, (c) m = 7 and (d) m = 13.

Furthermore, the switching angle α_m is equal to 60˚ when NP1 is equal to zero, for all values of m. The angular separation of the trajectories at the y-axis is can be defined as:

$$\text{Angular separation} = \frac{2\times 60^\circ}{m+1}, \text{ m is odd} \quad (3)$$

It can also be seen from Figure 3, for NP1 ranges from 0 to 0.8, the trajectories approximates a straight line. Hence a straight-line approximation of the trajectories could be used. However, for NP1 greater than 0.8, the trajectories are no longer straight lines. Nevertheless, the straight-line approximation could still be used with an error correction scheme for the region of NP1 greater than 0.8. Observing Figures 2a-d, the trajectories of the odd and the even switching angles are apparently parallel lines over most of the range of NP1. Also the slopes of the trajectories reduce with increasing values of m. Therefore, to obtain a relationship between the slopes of the trajectories for the different values of m, the slopes should first be normalized towards the angular separation of the trajectories. At NP1 = 0.8,

$$\text{Slope of the trajectories} = \frac{\frac{60^\circ(k+1)}{(m+1)} - \alpha_k}{0.8}, \text{fork odd} \quad (4)$$

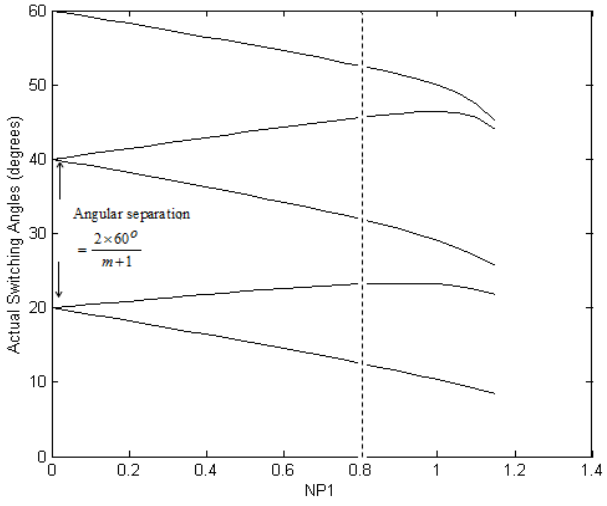

Figure 3. Trajectories for m = 5 to illustrate angular separation.

$$\text{Slope of the trajectories} = \frac{\alpha_k - \frac{60^\circ(k)}{(m+1)}}{0.8}, \text{ for k even} \quad (5)$$

Let Δ_k = normalized slope $\times 0.8$. Then

$$\Delta_k = \frac{\frac{60^\circ(k+1)}{(m+1)} - \alpha_k}{\frac{2\times 60^\circ}{m+1}}, \text{ for k odd} \quad (6)$$

$$\Delta_k = \frac{\alpha_k - \frac{60^\circ(k)}{(m+1)}}{\frac{2\times 60^\circ}{m+1}}, \text{ for k even} \quad (7)$$

Figure 4 shows the variation of Δ_k, for odd of k, for several values of m. The graphs suggest that for odd values of k, the function Δ_k is appears to be a polynomial (quadratic curves) with nearly constant amplitude. Therefore, the obvious solution would be to apply a quadratic polynomial fit to the curves in Figure 4. This leads the generalized equation for the odd values of Δ_k which will be of the form

$$\Delta_k = -\frac{0.21}{m^2}\left(k - \frac{m+1}{2}\right)^2 + 0.4025, \text{ for k odd} \quad (8)$$

The complete derivation of equations for the 2nd order polynomials approximated curves of the variation of Δ_k with k for odd values of k is shown in appendix A. The result is a generalized equation for the odd switching angles, for any value of m and NP1, is given by the equation below:

$$\alpha_k = \frac{60^\circ(k+1)}{m+1} - \left[\frac{2\times 60^\circ}{m+1} \times \frac{\Delta_k \times NP1}{0.8}\right], \text{ for k odd} \quad (9)$$

Figure 5 shows the variation of Δ_k for the even switching angles. Extrapolation shows that all the curves pass through the origin. For increasing values of m, the values of Δ_k appear to be asymptotic to a line drawn parallel to the x-axis and intersecting the y-axis at 0.325. Taking this into account, the generalized equation for the even

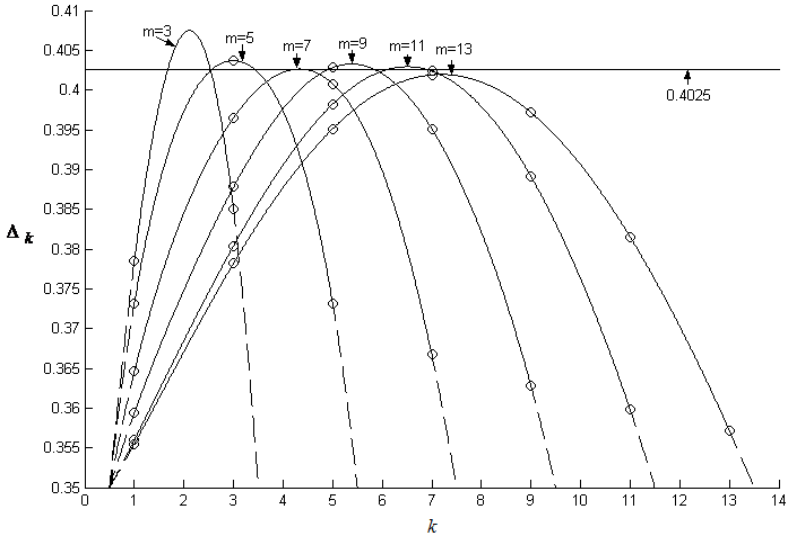

Figure 4. Variation of Δ_k towards k for several values of m (for odd k).

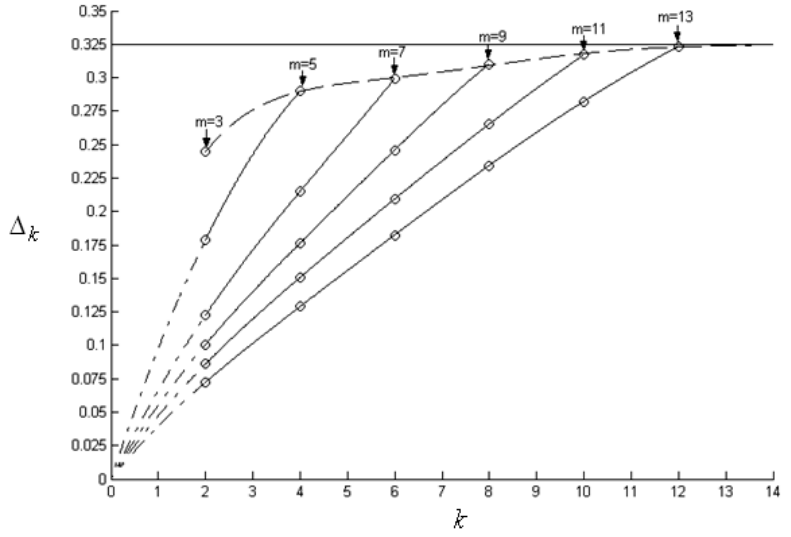

Figure 5. Variation of Δ_k towards k for several values of m (for even k).

values of Δ_k will be of the form given in the equation below:

$$\Delta_k = -\frac{0.082}{(m-1)^2}[k-2.482(m-1)]^2 + 0.505 - \frac{k}{m^3},$$

for k even (10)

The derivation of equations for the polynomial approximated curves of the variation of Δ_k with k for even values of k is as shown in Appendix B. The generalized algorithm for the even switching angles for any value of m and NP1, is then given by

$$\alpha_k = \frac{60^\circ \times k}{m+1} + \left[\frac{2\times 60^\circ}{m+1} \times \frac{\Delta_k \times NP1}{0.8}\right], \text{ for even k} \quad (11)$$

Equations 8-11 can now be used to calculate the approximate switching angles for any value of m

and NP1. These simple equations can be implemented easily on any microprocessor which has the multiplication command in its instruction set. The simplicity of the algorithm allows for very fast and efficient generation of the HEPWM waveform. The accuracy of the algorithm is investigated in the following section.

3. ACCURACY OF THE GENERALIZED ALGORITHM

The accuracy of the derived equations is evaluated by calculating the difference between the approximate switching angles from the proposed method and the exact switching angles from the trajectories. The latter are calculated using Newton-Raphson iteration method. The absolute difference is termed as the angle error. The angle errors relationship with NP1 and the k^{th} angle for values of m = 3, 5, 7, 9, 11 and 13, are shown in Figures 6a through 6f, respectively. For each of the six cases, the angle error trend is very small for NP1 < 0.8. In addition the errors reduce with the icreased values of m. However for values of NP1 > 0.8, the errors increase drastically. The reason for this can be attributed to the departure of the trajectories from being straight lines as can be seen earlier in Figures 2a-d. On this basis, for cases of NP1 > 0.8, a correction factor needs to be incorporated to the switching angles to reduce the error. The maximum angle errors for $0 < NP1 \le 0.8$ and $0.8 < NP1 \le 1.15$ are tabulated in Tables 1 and 2, respectively.

3.1. Error Correction. To account for the relatively large error for the case for $0.8 < NP1 \le 1.15$, an error correction factor is incorporated. For NP1 > 0.8, and k is odd,

$$\alpha_{k\,(corrected)} = \alpha_k - \Delta D_k \tag{12}$$

with

$$\Delta D_k = \frac{(NP1-0.8)^2}{0.09} \times \left[-\frac{52}{m}\left[\frac{k}{m+5} - 0.5 \right]^2 + \frac{13}{m} \right], \text{k odd} \tag{13}$$

While for even switching angles at NP1 > 0.8, the error correction factor is incorporated as before in the previous equation shown:

$$\alpha_{k(corrected)} = \alpha_k - \Delta D_k \tag{14}$$

with

$$\Delta D_k = \frac{(NP1-0.8)^2}{0.09} \times \left[-\frac{52}{m}\left[\frac{k}{m+3} - 0.5 \right]^2 + \frac{13}{m} \right], \text{k even} \tag{15}$$

The derivation of Equations 13 and 15 are shown in Appendix C.

Figures 7a through 7f show the absolute error between the exact switching angles and those calculated with the approximated HEPWM equations, incorporating the correction factors. Comparing Figure 6, it could be seen that the maximum errors have been reduced by a factor of 3-6 times. Table 3 shows the maximum errors at $0.8 < NP1 \le 1.15$ with and without error correction factor.

4. RESULTS AND DISCUSSION

To assess the effectiveness of the proposed HEPWM algorithm, a 200 W single phase VSI is constructed. The VSI is fed by 50V DC input voltage. The HEPWM is implemented in using a low-cost, fixed-point 16-bit Siemens 80C167 microcontroller. It has internal PWM modules for pulses generation. For comparison purposes, MATLAB simulation of the same VSI system is carried out. It is worth noting that since the resolution of the PWM module in the microcontroller is 400 ns, deviations from theoretical results are expected. In addition, the effect of the 1μs dead time introduced to each switching pulse is not considered. Clearly both factors affect the accuracy significantly, particularly at high value of m where the HEPWM pulses are nearing their minimum widths.

4.1. Cases for NP1 < 0.8 Figures 8a,b show the output voltage waveform of the VSI at NP1 = 0.7 for m = 5 and m = 9, respectively. For m = 5, the expected eliminated harmonics (besides the triplens) are the 5^{th}, 7^{th}, 11^{th} and 13^{th}, while for m = 9

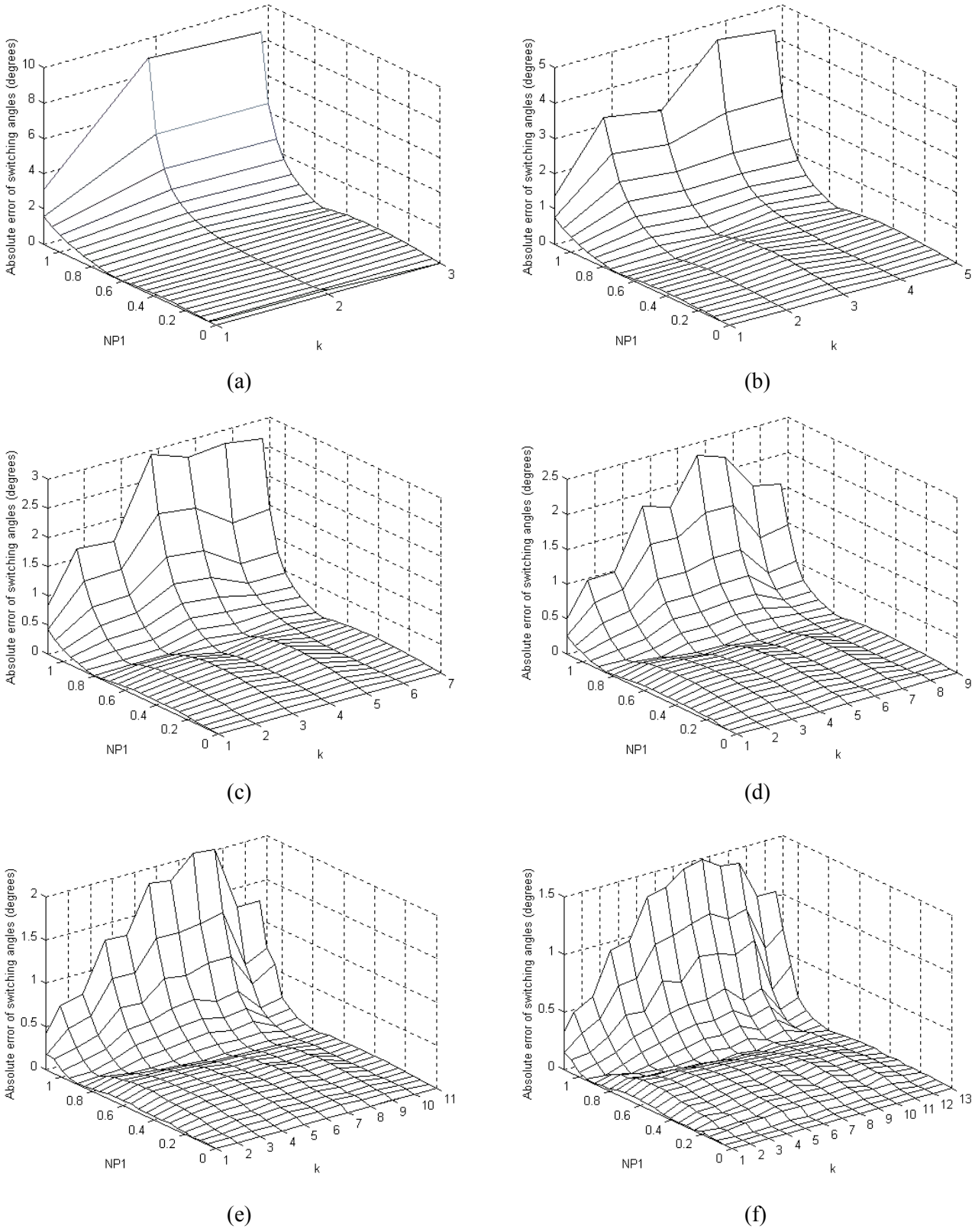

Figure 6. Variation of switching angle errors for (a) m = 3, (b) m = 5, (c) m = 7, (d) m = 9, m = 11, (e) m = 11 and (f) m=13.

TABLE 1. Maximum Errors in Switching Angles for $0 < NP1 \leq 0.8$ **.**

m	Maximum Error for Odd Switching Angles (Degree)	Maximum Error for Even Switching Angles (Degree)
3	0.6795	0.8967
5	0.3242	0.4535
7	0.2759	0.3469
9	0.2136	0.2232
11	0.1784	0.1582
13	0.1533	0.1154

TABLE 2. Maximum Errors in Switching Angles for $0.8 < NP1 \leq 1.15$ **.**

m	Maximum Error for Odd Switching Angles (Degree)	Maximum Error for Even Switching Angles (Degree)
3	8.3785	8.6192
5	4.2015	4.3793
7	2.6184	2.8355
9	2.2420	2.1003
11	1.9446	1.9688
13	1.4446	1.4038

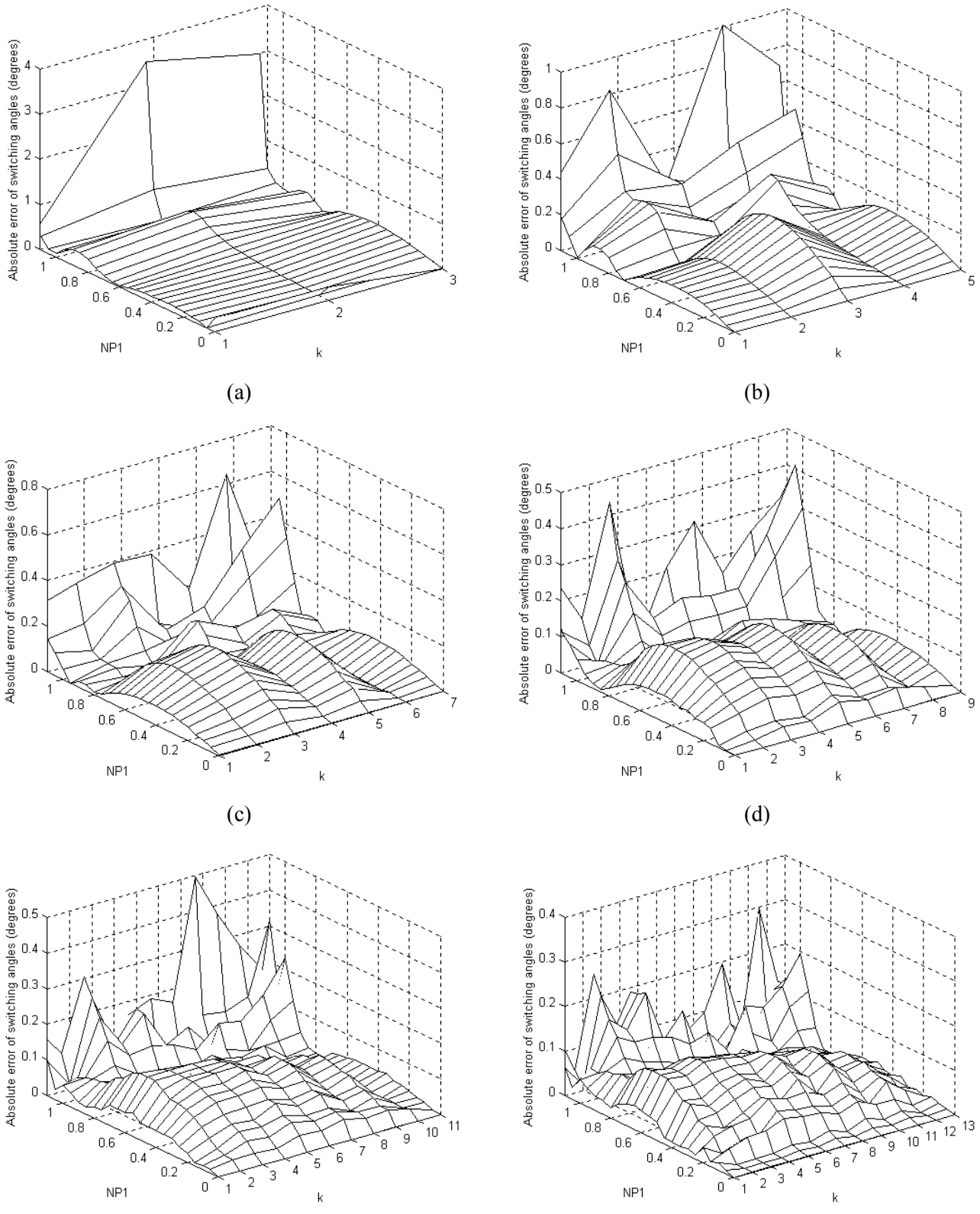

Figure 7. Variation of error, incorporating error correction for NP1 > 0.8 (for m=3,5,7,9,11,13).

TABLE 3. Maximum Error in Switching Angles with and Without Error Correction for $0.8 < NP1 \leq 1.15$.

	Without Correction		With Correction	
m	Max. Error for Odd Switching Angles (Degree)	Max. Error for Even Switching Angles (Degree)	Max. Error for Odd Switching Angles (Degree)	Max. Error for Even Switching Angles (Degree)
3	8.3785	8.6192	2.8490	3.3764
5	4.2015	4.3793	0.6626	0.9819
7	2.6184	2.8355	0.3697	0.6173
9	2.2420	2.1003	0.4186	0.2294
11	1.9446	1.9688	0.3606	0.4798
13	1.4446	1.4038	0.2411	0.2844

the additional eliminated harmonics are 17^{th}, 19^{th}, 23^{rd} and 27^{th}. Figures 9a,b show the spectra plots of Figures 8a,b computed using the FFT function of the oscilloscope. With a frequency axis scaled at 250 Hz/div, it can be observed that all the specified harmonics are successful eliminated. For a three phase systems, since all triplens are absent, the first un-eliminated harmonic is located at (3m+2). Thus if m = 5, first harmonic exists at 17^{th} or at 850Hz for 50Hz fundamental frequency. For m = 9, the first harmonic appears at 31^{st}. It is important to note in the spectra of Figure 9a, the first remaining harmonic (i.e. the 17^{th}) has a large magnitude. This is a particular characteristic of HEPWM, where the energy that would have been associated with those eliminated harmonics is transferred to the first remaining harmonic, considerably increasing its amplitude [15]. Figures 10 a,b show the spectral plots for cases m = 7 and 13, respectively.

4.2. Cases for NP1 > 0.8 For NP1 > 0.8, the eliminated harmonics is expected to reappear due to the non-linearity portion of the trajectories curves. To overcome this, a correction factor is incorporated into the HEPWM switching angle as described by Equations 12-15. Figure 11a shows the spectra of the output voltage without the correction factor for m = 7 at NP1 = 1.1. Careful observation reveals the eliminated harmonics reappear at 5^{th}, 7^{th}, 11^{th}, 13^{th} and 17^{th} and 19^{th}. Figure 11b shows the resulting spectra after the correction factor is included. As can be seen, the magnitudes of the harmonics that reappear are reduced significantly.

However it can also be noted that the amplitudes of the remaining (un-eliminated) harmonics increase slightly. Figures 12a,b show the performance of the first four eliminated harmonics for values of m up to 17. From these figures it can be learned that by incorporating the correction factor, the performance has been improved between 4 to 6 times.

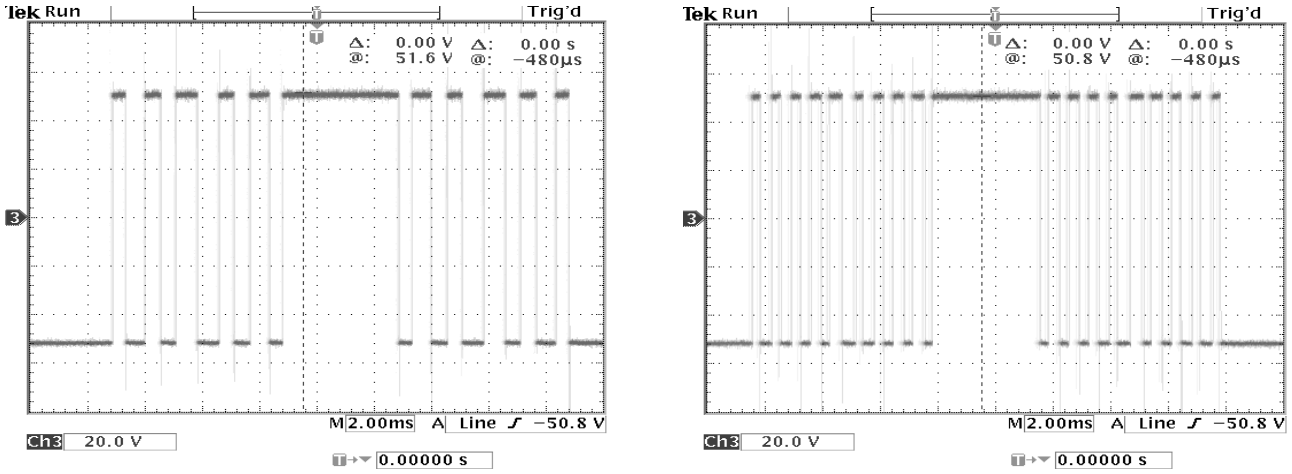

(a) (b)

Figure 8. VSI output waveform an NP1 = 0.7, fundamental frequency = 50 Hz, (a) m = 5 and (b) m = 9.

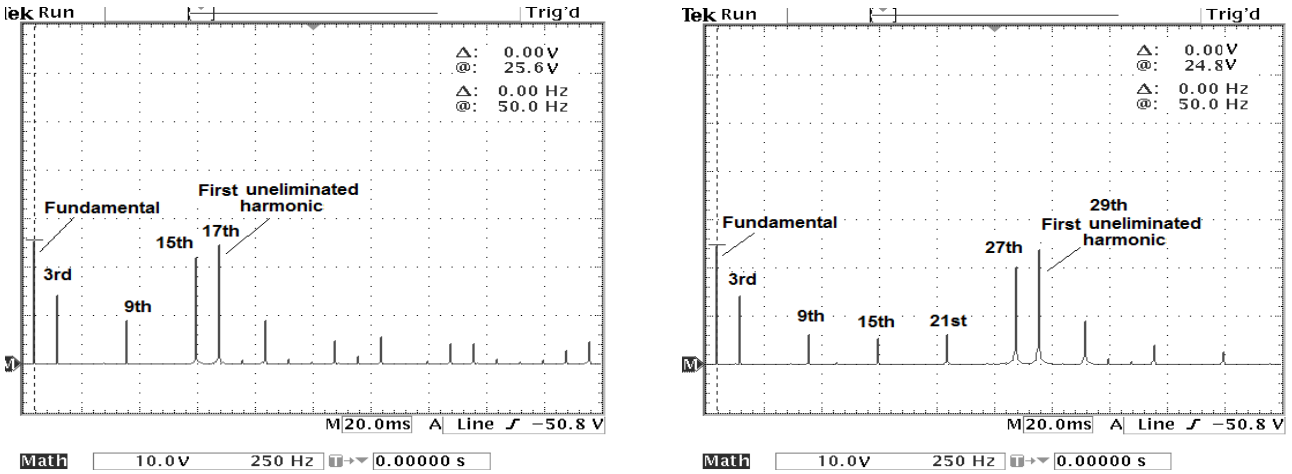

(a) (b)

Figure 9. Spectra of VSI output at NP1 = 0.7, fundamental freqrequency= 50 Hz (a) m = 5 and (b) m=9. Scale: Amplitude (y-axis): 10 V/div. Frequency (x-axis): 250 Hz/div. Note that all triplens become zero when line to line voltage of a three phase VSI is considered.

5. CONCLUSION

This paper proposed an efficient and fast on-line algorithm to calculate the switching angles of HEPWM. It is based on the polynomial curve fittings that approximate of the trajectories of the exact HEPWM switching angles. It results in generalized equations which require only the addition and multiplication processes allowing its implementation using a low cost microprocessor. Changes to the number of harmonics to be eliminated and the fundamental amplitude of the pole switching waveform (NP1) can be calculated independently. This feature is particularly suited for motor drive application. An extensive analysis to determine the accuracy of the algorithm is carried out. To verify the workability of the technique, an experimental single phase test rig was constructed. The algorithm is implemented using a fixed point, 16-bit microprocessor. The

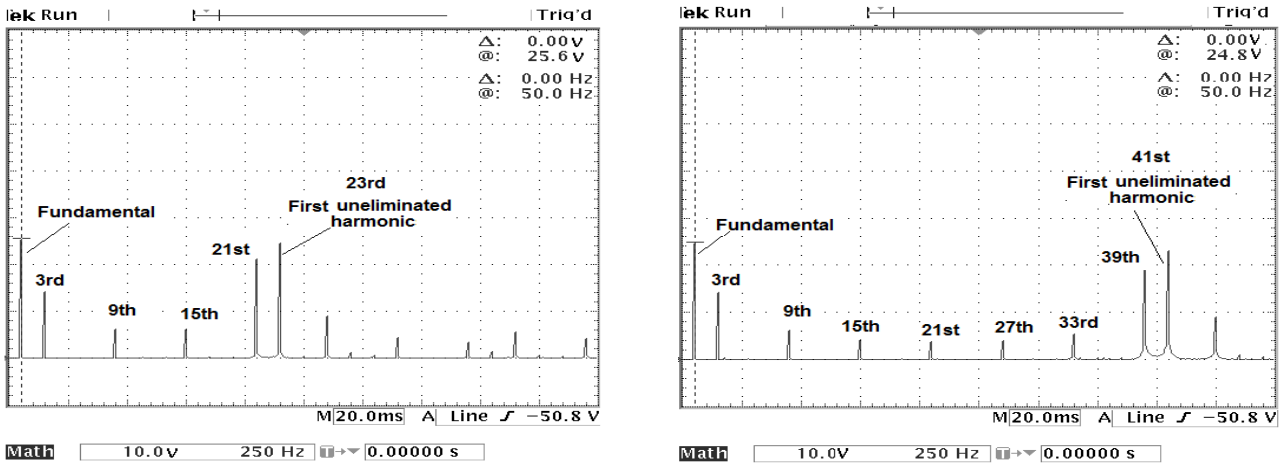

(a) (b)

Figure 10. Spectra of VSI output at NP1 = 0.7, fundamental frequency = 50 Hz. (a) m = 7 and (b) m = 13. Scale: Amplitude (y-axis): 10 V/div. Frequency (x-axis): 250 Hz/div.

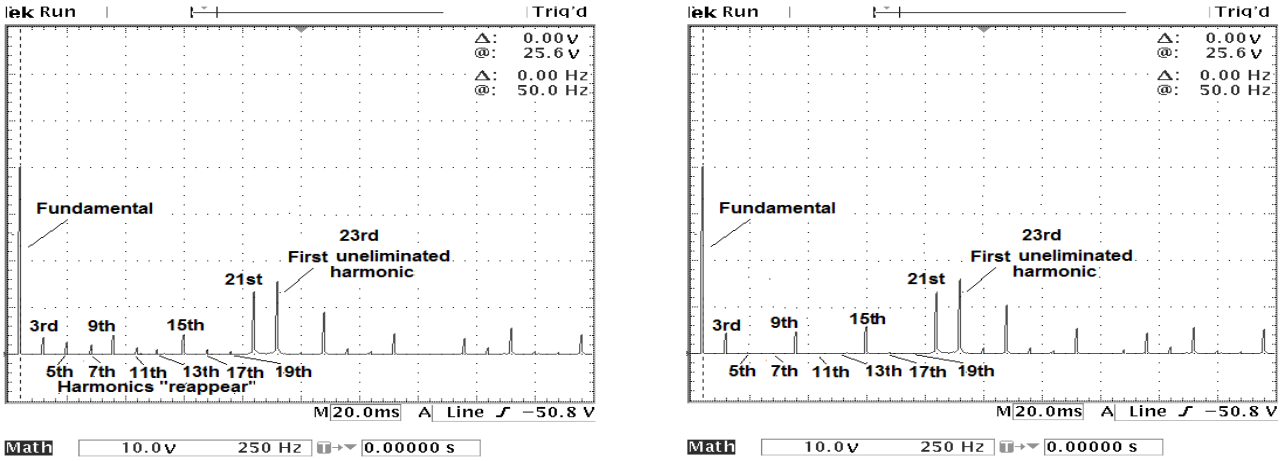

(a) (b)

Figure 11. Spectra with m = 7, NP1 = 1.1, (a) without correction factor and (b) with correction factor. Scale: Amplitude (y-axis): 10 V/div. Frequency (x-axis): 250 Hz/div. Note that all triplens become zero when line to line voltage of a three phase VSI is considered.

result obtained from the test rig is in good agreement with the theoretical prediction.

6. APPENDIX

6.A. Derivation of Switching Angle Equation for Odd k From Figure 4, a suitable equation for the curves using the quadratic fit would be

$$\Delta_k = -a(k-b)^2 + c \qquad \text{(A1)}$$

From the same figure the following constants are obtained:

$$c = 0.4025 \qquad \text{(A2)}$$

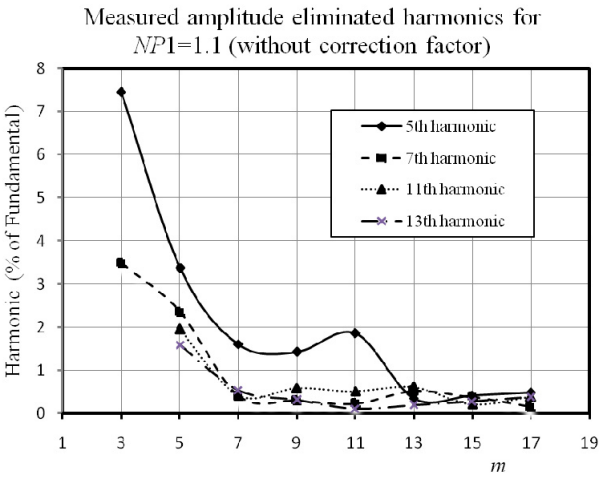

(a)

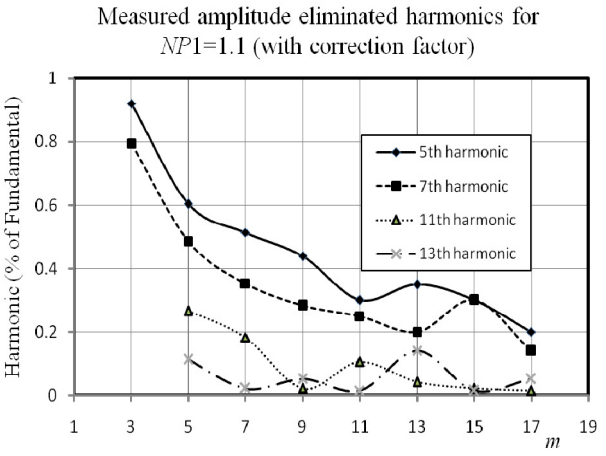

(b)

Figure 12. Measured values of the first four eliminated harmonics for different m values at NP1=1.1, (a) without correction factor and (b) with correction factor.

$$b = \frac{m}{2} + 0.5 = \frac{m+1}{2} \quad \text{(A3)}$$

$$\Delta_k = 0.35 \text{ at } k = 0.5 \quad \text{(A4)}$$

Substitute (A1), (A2) and (A3) in (A1),

$$0.35 = -a\left(0.5 - \frac{m+1}{2}\right)^2 + 0.4025$$

$$a = \frac{0.21}{m^2} \quad \text{(A5)}$$

Substitute (A2), (A3) and (A5) in (A1),

$$\Delta_k = -\frac{0.21}{m^2}\left(k - \frac{m+1}{2}\right)^2 + 0.4025, \text{ for odd k} \quad \text{(A6)}$$

With a straight line approximation, Δ_k will reduce linearly to zero at NP1 = 0. Thus, the generalized algorithm for the odd switching angles, for any value of m and NP1, is given by the equation below:

$$\alpha_k = \frac{60^\circ(k+1)}{m+1} - \left[\frac{2\times 60^\circ}{m+1} \times \frac{\Delta_k \times NP1}{0.8}\right], \text{ for k odd} \quad \text{(A7)}$$

6.B. Derivation of Switching Angle Equation for Even k From Figure 5, a suitable equation for the curves using the quadratic fit would be of the form

$$\Delta_k = -a(k-b)^2 + c \quad \text{(B1)}$$

It could be seen that Δ_k = 0.325 for m = 13 and above. With Δ_k = 0.325 and k = m1,

$$0.325 = -a(m-1-b)^2 + c \quad \text{(B2)}$$

While $k = \frac{m-1}{2}$ for every curve, Δ_k is found to be very near the value of 0.183. Using these information,

$$0.183 = -a\left(\frac{m-1}{2} - b\right)^2 + c \quad \text{(B3)}$$

Since Δ_k = 0 at k = 0, then

$$0 = -ab^2 + c \quad \text{(B4)}$$

Subtract (B4) from (B2),

$$0.325 = -a\left[(m-1-b)^2 - b^2\right]$$

From

$$a^2 - b^2 = (a+b)(a-b), \; 0.325 = -a(m-1)(m-1-2b) \quad \text{(B5)}$$

Subtract (B4) from (B3),

$$0.183 = -a\left[\left(\frac{m-1}{2} - b\right)^2 - b^2\right]$$

From

$$a^2 - b^2 = (a+b)(a-b),$$

$$0.183 = -a\left(\frac{m-1}{2}\right)\left(\frac{m-1}{2} - 2b\right)$$

$$0.366 = -a(m-1)\left(\frac{m-1}{2} - 2b\right) \quad \text{(B6)}$$

Divide (B5) with (B6),

$$0.888 = \frac{(m-1-2b)}{\frac{m-1}{2} - 2b}$$

$$b = 2.482(m-1) \quad \text{(B7)}$$

Substitute (B7) in (B5),

$$0.325 = -a(m-1)(m-1-2(2.482)(m-1))$$

$$a = \frac{0.082}{(m-1)^2} \quad \text{(B8)}$$

Substitute (B7) and (B8) in (B4),

$$0 = -\left[\frac{0.082}{(m-1)^2}(2.482(m-1))^2\right] + c$$

$$c = 0.505 \quad \text{(B9)}$$

Substitute (B7), (B8) and (B9) in (B1) yields:

$$\Delta_k = -\frac{0.082}{(m-1)^2}[k - 2.482(m-1)]^2 + 0.505 \quad \text{(B10)}$$

The generalized algorithm for the even switching angles for any value of m and NP1, is then given by:

$$\alpha_k = \frac{60^\circ \times k}{m+1} + \left[\frac{2\times 60^\circ}{m+1} \times \frac{\Delta_k \times NP1}{0.8}\right],$$

for even k (B12)

6.C. Error Correction Method As could be seen for NP1 greater than 0.8, the errors in the switching angles increase nonlinearly for each value of m and the maximum error for each value of m increases with reducing m. To account for this, an adjusted error correction factor is defined as in equation (C1), at particular amplitude of NP1 and for various values of m.

$$\Delta E_k = m\Delta D_k \quad \text{(C1)}$$

Where

$$\Delta D_k = \alpha_k \text{approximate} - \alpha_k \text{accurate} \quad \text{(C2)}$$

Figures C1 and C2 show the variation of ΔE_k, for odd and even values of k, at an amplitude of NP1 = 1.1.

From Figure C1, a suitable equation for the curves using the quadratic fit would be,

$$\Delta E_k = -a(k-b)^2 + c \quad \text{(C3)}$$

Where

$$c = 13,\ b = \frac{m+5}{2}$$

and

$$\Delta E_k = 0 \text{ at } k = 0$$

Substitute these in (C3) results in

$$\Delta E_k = -\frac{52}{(m+5)^2}\left[k - \frac{m+5}{2}\right]^2 + 13 \quad \text{(C4)}$$

$$\Delta E_k = -52\left[\frac{k}{m+5} - 0.5\right]^2 + 13 \quad \text{(C5)}$$

Since

$$\Delta E_k = m\Delta D_k,$$

$$\Delta D_k = -\frac{52}{m}\left[\frac{k}{m+5} - 0.5\right]^2 + \frac{13}{m}$$

for odd k at NP1 = 1.1 (C6)

From Figure C2, the graphs also appear to approximate quadratic curves, so the best possible

fit again will be a quadratic fit. A suitable equation for the curves using the quadratic fit would be,

$$\Delta E_k = -a(k-b)^2 + c \qquad (C7)$$

From the figure:

$$c = 13\,,\ b = \frac{m+3}{2}$$

and

$$\Delta E_k = 0 \ \text{ at } k = 0$$

Substitute these into (C7) result in,

$$\Delta E_k = -\frac{52}{(m+3)^2}\left[k - \frac{m+3}{2}\right]^2 + 13 \qquad (C8)$$

$$\Delta E_k = -52\left[\frac{k}{m+3} - 0.5\right]^2 + 13 \qquad (C9)$$

Since

$$\Delta E_k = m\Delta D_k\,,$$

$$\Delta D_k = -\frac{52}{m}\left[\frac{k}{m+3} - 0.5\right]^2 + \frac{13}{m}$$

for even k at NP1 = 1.1 (C10)

Assuming that the variation of ΔD_k with the amplitude of NP1 is given accurately enough by the nonlinear expression shown in Figure C3, the generalized equation for ΔD_k, for NP1 greater than 0.8 is as given below,

$$\Delta D_k = \frac{\left(\Delta D_k\right)_{1.1}}{0.09}(NP1 - 0.8)^2 \qquad (C11)$$

Therefore

$$\Delta D_k = \frac{(NP1-0.8)^2}{0.09} \times \left[-\frac{52}{m}\left[\frac{k}{m+5} - 0.5\right]^2 + \frac{13}{m}\right],$$

for k odd (C12)

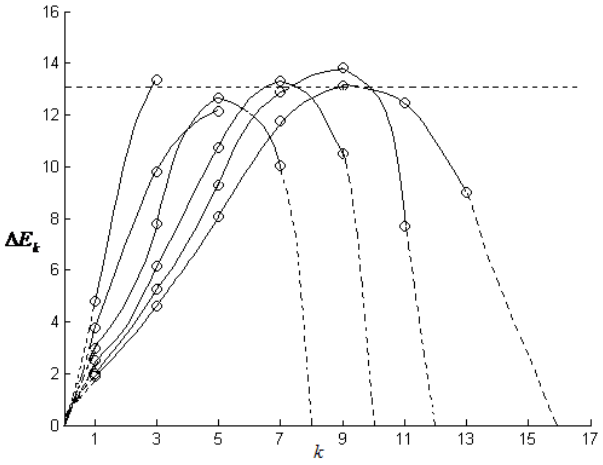

Figure C1. Variation of ΔE_k with k (for odd values of k).

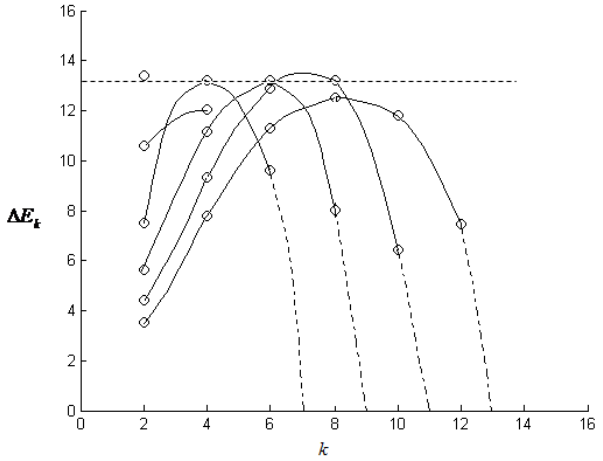

Figure C2. Variation of ΔE_k with k (for even values of k).

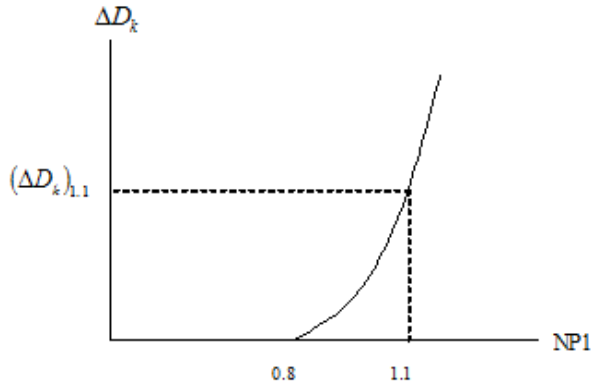

Figure C3. Variation of ΔD_k with NP1.

$$\Delta D_k = \frac{(NP1 - 0.8)^2}{0.09} \times \left[-\frac{52}{m}\left[\frac{k}{m+3} - 0.5\right]^2 + \frac{13}{m} \right],$$

for k even (C13)

7. REFERENCES

1. Hasmukh, H., Patel, S. and Hoft, R.G., "Generalized Techniques of Harmonic Elimination and Voltage Control in Thyristor Inverters: Part I-Harmonic Elimination", ***IEEE Transaction on Industrial Applications***., Vol. IA-9, No. 3, (1973), 310-317.
2. Hasmukh, H. Patel, S. and Hoft, R.G., "Generalized Harmonic Elimination and Voltage Control in Thyristor Inverters: Part II—Voltage Control Technique", ***IEEE Transaction on Industrial Applications***., Vol. IA-10, No. 5, (1974), 666-673.
3. Enjeti, P. and Lindsay, J.F., "Solving Nonlinear Equations of Harmonic Elimination PWM in Power Control", ***Electronics Letters***, Vol. 23, No. 12, (Jun 1987), 656-657.
4. Enjeti, P., Ziogas, P.D. and Lindsay, J.F., "Programmed PWM Techniques to Eliminate Harmonics: A Critical Evaluation", ***IEEE Transaction on Industry Applications***., Vol. 26, No. 2, (June 2000), 245-2533.
5. Taufiq, J.A., Mellitt, B. and Goodman, C.J., "Novel Algorithm for Generating Near Optimal PWM Waveforms for AC Traction Drives", ***IEE Proceedings***, Vol. 133, No. 2, (1986), 85-93.
6. Bowes, S.R. and Clark, P.R., "Simple Microprocessor Implementation of New Regular-Sampled Harmonic Elimination PWM Techniques", ***IEEE Transaction on Industry Applications***., Vol. 28, No. 1, (1992), 89-95.
7. Bowes, S.R. and Grewal, S., "Novel Space-Vector-Based Harmonic Elimination Inverter Control", ***IEEE Transactions on Industry Applications***, Vol. 36, (March-April 2000), 549-557.
8. Agelidis, V.G., Balouktsis, A. and Balouktsis, I., "On Applying a Minimization Technique to the Harmonic Elimination PWM Control: The Bipolar Waveform", ***IEEE Power Electronics Letters***, Vol. 2, No. 2, (June 2004), 41-44.
9. Liang, T.J., O'Connell, R.M. and Hoft, R.G., "Inverter Harmonic Reduction using Walsh Function Harmonic Elimination Method", ***IEEE Trans. on Power Electronics***, Vol. 12, (November 1997), 971-982.
10. Kato, T., "Sequential Homotopy-Based Computation of Multiple Solutions for Selected Harmonic Elimination in PWM Inverters", ***IEEE Transactions on Circuits and Systems I: Fundamental Theory and Applications***, Vol. 46, (May 1999), 586–593.
11. Chiasson, J.N., Tolbert, L.M., McKenzie, K.J. and Zhong, D., "Elimination of Harmonics in a Multilevel Converter using the Theory of Symmetric Polynomials and Resultants", ***IEEE Transactions on Control Systems Technology***, Vol. 13, (March 2004), 216-223.
12. Zhong, D., Tolbert, L.M. and Chiasson, J.N., "Active Harmonic Elimination for Multilevel Converters", ***IEEE Transactions on Power Electronics***, Vol. 21, (March 2006), 459-469.
13. Tolbert, L.M., Chiasson, J.N., Zhong, D. and McKenzie, K.J., "Elimination of Harmonics in a Multilevel Converter with Nonequal DC Sources", ***IEEE Transactions on Industry Applications***, Vol. 41, (January-February 2005), 75-82.
14. Ozpineci, B., Tolbert, L.M. and Chiasson, J.N., "Harmonic Optimization of Multilevel Converters using Genetic Algorithms", ***IEEE Power Electronics Letters***, Vol. 3, (September 2005), 92-95.
15. Bowes, S.R. and Holliday, D., "Optimal Regular-Sampled PWM Inverter Control Techniques", ***IEEE Transactions on Industrial Electronics***, Vol. 54, (June 2007), 1547–1559.